

# **IRON OXIDE NANOPARTICLES AS A NOVEL MAGNETICALLY GUIDED TARGETED THERAPY FOR BREAST CANCER TREATMENT**

## **1. Introduction**

Cancer is considered as a significant cause of death worldwide. The initiation of cancer is very fast and can rapidly spread to the other healthy cells and tissues of the body. Among various cancers, breast cancer is considered as the second most cause of death globally. Breast cancer accounts for about 14% of cancer in Indian women. A report on breast cancer statistics has confirmed that the new breast cancer cases had risen to more than 22 lakhs in 2020, and the death rate was estimated as 87,090 [1]. Conventional chemotherapeutic drugs experience some limitations in distinguishing between normal and cancerous cells, leading to systemic toxicity and severe side effects [2].

Triple-Negative Breast Cancer (TNBC) is a type of breast cancer that is aggressive and prone to rapid multiplication at the lymph nodes and has a higher chance of recurrence [3]. Once cancer spreads to the lymph nodes or other parts of the body the chances of survival rate of a patient is greatly reduced. It has been reported that the TNBC can grow very faster and eventually spread to a great extent at the time of its diagnosis [4]. As the three prominent women's hormonal receptors (Progesterone, Estrogen and Human epidermal growth factor) are not present in TNBC, hormone therapy or immunotherapy are excluded from the list of treatments for TNBC. Hence chemotherapy using taxanes, anthracyclins, PARP inhibitors, etc. remains the major treatment against TNBC. Unfortunately, inherited cytotoxic activity, non-targeted delivery, and higher doses of these chemotherapeutic drugs result in severe systemic side effects and poor prognosis and the destruction of a large number of healthy cells compared to the TNBC cells. Therefore, it is the high time to implement advanced and novel strategies like nanotechnology in the treatment and control of TNBC [5].

In the last few decades, the demand for nanoparticles in the bio-pharmaceutical application has risen tremendously. Among various nanoparticles, Iron oxide nanoparticles (IONPs) is considered as the most efficient in cancer diagnosis and treatment due to some specific physical and chemical properties. IONPs has so many unique features like superparamagnetism, good tissular diffusion, and better bioavailability with low toxicity. In this regard, IONPs are gaining popularity in various biomedical fields due to their effective size control phenomena, surface characterization along with unique superparamagnetism property [6], [7]. In recent years, the IONPs based nano-medicines have been applied for advanced detection, diagnosis, treatment and control of breast cancer related deaths [8],

[9]. Additionally, due to their superparamagnetic property the surface coated iron oxide nanoparticles can be easily directed towards the specific target site by aid of an external magnetic field with increased efficacy and reduced side effects of chemotherapeutic drugs.

As per the latest trend of their synthesis process the green chemistry technique can replace the use of external chemicals by providing naturally available reducing, capping agents for the reduction of the iron ions [1].

The Triphala churna (powder) affirms the presence of many valuable phytoconstituents such as gallic acid, ellagic acid, chebulinic acid, L-ascorbic acid, alkaloids, bellaricanin, beta-sitosterol, flavonoids (Quercetin, Luteolin etc), saponins, amino acids and so forth which shows strong antioxidant and anticancer activities[16]. Recently, Triphala has also demonstrated potent anticancer activity in HeLa (cervical adenocarcinoma), PANC-1 (pancreatic adenocarcinoma), and MDA-MB-231 (triple-negative breast carcinoma) cells[17]. Prasad et al. observed that the treatment with the aqueous extract of Triphala churna reduces cell proliferation of breast and prostate cancer cells [18]. They suggested that the anticancer activity of Triphala churna is contributed by its polyphenols, ascorbic acid and flavonoids. In another investigation, the anti-proliferative impact of Triphala extract act against MCF-7 breast cancer cell line was reported [19]. In spite of these promising reports about the anticancer activity of Triphala churna in breast cancer, including TNBC, the direct administration of crude Triphala churna to the cancer patients may be proven ineffective due to the poor bioavailability of its active phytoconstituents from the powdered mixture of its herbal ingredients as well as it may be inconvenient to administer in such patients [20,21].

The main objective of this present study is to develop IONPs to be applicable for breast cancer treatment and reduce the side effects of chemotherapeutic drugs. As per our first protocol, the IONPs was prepared using green synthesis method from Triphala churna extract (TIONPs) to evaluate its anticancer efficacy in treating TNBC. In the next approach IONPs with superparamagnetic property will be prepared to evaluate the targeted drug delivery of doxorubicin at the breast cancer site using external magnet.

## 2. Objectives

- To formulate Iron oxide nanoparticles using green synthesis technique from aqueous extract of Triphala churna (TIONPs) and evaluate its in-vitro cytotoxic activity
- To develop doxorubicin loaded PVA coated superparamagnetic IONPs(Dox-IONPs) for targeted drug delivery at breast cancer site using external magnetic field
- To commercialize the formulated IONPs in the market as a promising therapeutic carrier for the breast cancer treatment

## 3. Materials and methods

### 3.1. Materials

Ferric chloride hexahydrate ( $\text{FeCl}_3 \cdot 6\text{H}_2\text{O}$ , purity ~98%), Amlaki (*Embellica officinalis*), Haritaki (*Terminalia chebula*), and Bibhitaki (*Terminalia bellirica*), 4',6-Diamidino-2-phenylindole dihydrochloride (DAPI), Paraformaldehyde, Dimethyl sulfoxide (DMSO), Methylthiazolyldiphenyl-tetrazolium bromide (MTT), Trypan blue solution, and Fluoromount-G were obtained from Himedia Labs (India). Acridine orange (AO)

### 3.2. Methods

#### 3.2.1. Development and establishment of cytotoxic potential of IONPs from triphala extract using green synthesis technique

##### 3.2.1.1. Preparation of aqueous extract of Triphala churna

All three herbal ingredients were subjected for grinding followed by sieving through sieve size 60 and mixing in equal proportion to obtain the Triphala churna. The aqueous extract of the churna was prepared by immersing one gram of finely ground product into 100 mL distilled water and heating it up to 70 °C for 30 min in a temperature-controlled water bath. The resulting extract was allowed to cool and filtered through Whatman filter paper to remove the debris. Finally, the cleared extract was stored under refrigeration for further use.

##### 3.2.1.2. Characterization of the Triphala churna extract

###### i. Total Phenolic Content (TPC)

The aqueous extracts of the Triphala churna and its three ingredients were evaluated separately for the determination of total phenol content according to the Folin–Ciocalteu method using gallic acid as reference standard [22]. Briefly, 1 mL of the different concentration of the extract or gallic acid was mixed with 1 mL of Folin–Ciocalteu reagent and 1 mL of sodium carbonate (2% w/v). The mixture was incubated for 1h at room

temperature and the absorbance was recorded using UV-Vis double beam spectrophotometer against a blank at 765 nm. The total phenolic content in mg GAE/g in the extract was calculated (Mean  $\pm$  S.D., n=3) by the help of the Gallic acid standard curve (50-500 $\mu$ g/mL).

ii. *Total Flavonoid content (TFC)*

In a clean test tube, 1 mL of the extract was taken along with 4 mL of distilled water and then 0.3 mL of sodium nitrite (5% w/v) was added to it. After 10 min, 0.3 mL aluminium chloride (10% w/v), and 2 mL of 1M sodium hydroxide were added. The total volume was made up to 10 mL with distilled water with thorough mixing. The absorbance reading was recorded at 510 nm with the help of a UV-Vis spectrophotometer. Total flavonoid content (mg QE/g) was estimated with the help of the quercetin standard curve (25-100  $\mu$ g/mL) similar to TPC method [23].

iii. *HPTLC fingerprinting*

The aqueous extracts of Triphala churna and its all three components were applied on a pre-coated silica gel 60F<sub>254</sub> Aluminium plate (10 cm  $\times$  10 cm) with 0.2 mm thickness by the Linomat 5 sample application system (CAMAG) [24]. The plate was then placed in CAMAG glass twin trough developing chamber previously saturated with the mobile phase of Toluene: Ethyl acetate: Formic acid: Methanol (3: 2.6: 0.4: 4). The developed plate was dried and the retention factor ( $R_f$ ) values of the developed spots were noted under specified wavelengths (254 nm, 366 nm and 540 nm). The High performance thin layer chromatography (HPTLC) finger print data were documented by winCAT software (CAMAG).

**3.2.1.3. Green synthesis of Triphala mediated Iron oxide nanoparticles (TIONPs)**

Ferric chloride hexahydrate (FeCl<sub>3</sub>.6H<sub>2</sub>O) was used as precursor salt to synthesize TIONPs. The specific amounts of Ferric chloride hexahydrate (1 mM) was directly added to the 100 mL of aqueous churna extract (10 mg/ml) with a constant stirring at 600-700 rpm by a magnetic stirrer at room temperature. The pH of the mixture was adjusted to 11 by adding alkali solution, and the reaction mixture was constantly stirred for 30 min for complete synthesis. Gradually, the colour was changed from reddish-orange to intense black, which confirmed the formation of TIONPs. After completing the synthesis, the solution was centrifuged at 12000 rpm for 20 min and cleansed by repeated washing with distilled water 2-3 times to remove the impurities. The nanoparticles were collected in a pellet form and dried

in a hot air oven at 60 °C for 3 h and stored in a tube for further use. Finally, the percentage yield of synthesized TIONPs was calculated as per the standard method [25]

#### ***3.2.1.4. Analytical characterization of TIONPs***

The characterization of optimized TIONPs was done by various analytical techniques to assure their size/particle size distribution, shape, porosity, aggregation, zeta potential, surface chemistry, crystallinity, colloidal stability, etc. The optical property and completion of reduction of the iron ion was ensured with the help of a double beam spectrophotometer UV-Visible spectroscopy (JASCO V-630 Spectrophotometer) by recording the absorbance spectra. The total iron content in the TIONPs sample was estimated by Atomic absorption spectrometer (Systronics India Ltd, AAS-816) fixed at 248 nm using the calibration curve of ferrous chloride (0.25- 1 mg/L) [26]. The functional group detection was conducted by FTIR spectrometer (Jasco-4200, USA) using the KBr pellet method, where the scanning range was kept from 4000 to 400 cm. X-ray Diffraction (XRD) analysis was performed in the  $2\theta$  range between 20°-80° with Cu-K radiation and  $\lambda = 1.5406 \text{ \AA}$  for the determination of their surface characteristics along with the average particle size. The surface morphology of the compounds was determined using Scanning Electron Microscopy (SEM, NOVA NANOSEM 450). The particle size and zeta potential of the synthesized nanoparticles were determined using the principle of dynamic light scattering using Zetasizer 3600 (by Malvern Instruments Ltd. UK). Quantum design Evercool SQUID-VSM (MPMS 3) was employed at room temperature with the varying magnetic field from -10 to +10 kOe to determine of the magnetic property of produced iron oxide nanoparticles.

#### ***3.2.1.5. Evaluation of in-vitro antioxidant and anti-inflammatory activities***

The in-vitro antioxidant activity was evaluated using an ascorbic acid standard by 1, 1-diphenyl-2-picrylhydrazyl (DPPH) free radical scavenging method. Briefly, 2 ml of DPPH methanolic solution (0.1 mM) was mixed thoroughly with the 3 mL of different concentrations (1, 5, 7, 10, 30, 50, and 100 µg/ml) of churna extract or TIONPs solution and incubated at the dark condition for 30 min. Thereafter, the absorbance was recorded at 517 nm in UV-Vis spectrophotometer, and the IC<sub>50</sub> value was calculated from the ascorbic acid standard curve [27].

The in-vitro anti-inflammatory assay was carried out by the previously reported protein denaturation method [28]. Briefly, 0.02 mL of different concentrations 5 -100 µg/ml sample (Triphala churna extract or synthesized TIONPs) solution was mixed thoroughly with 0.2 ml

aqueous solution of bovine serum albumin (BSA) (1% W/V) and 4.8 ml of phosphate buffer solution (PBS, pH 6.4). Then they were incubated for 20 min at room temperature and followed by heating at 57 °C for 20 min. Thereafter, the samples were allowed to cool and the turbidity was measured using UV-Vis spectrophotometry at 660 nm. Percentage inhibition of protein denaturation was calculated in comparison with Diclofenac sodium as a standard drug.

### ***3.2.1.6. Cell lines and in-vitro cytotoxicity study of TIONPs***

Human triple-negative breast cancer cell line MDA-MB-231 and human skin cancer cell line A431 were procured from National Centre for Cell Sciences (NCCS, Pune, India). Murine breast cancer cell lines, 4T1 and Human embryonic kidney cells (HEK-293), were procured from the American Type Culture Collection (ATCC, USA). Dulbecco's Modified Eagle *Medium* (DMEM), Minimum Essential Medium Eagle (MEM), Penicillin streptomycin, Trypsin-EDTA, and Fetal bovine serum (FBS) were purchased from Himedia Labs (India).

#### ***i. MTT assay***

MTT Assay was performed to determine the cell viability of the TIONPs on different cell lines such as TNBC cell lines (MDA MB231, 4T1), Skin cancer cell line (A431), and normal healthy cell line (HEK 293) using 96 well plates. At first, 100 µl of the cell suspension was added into each well with a concentration of 10,000 cells per well. The plates were incubated in 5% CO<sub>2</sub> at 37°C for 24 h followed by addition of formulated TIONPs at various concentration (15.62, 31.25, 62.5, 125, 250 and 500 µg/ml). Thereafter, the cells were again incubated for 24 h or 48 h. After this treatment period, 50 µl of MTT reagent (5 mg/ml) prepared in sterile PBS was added into each well and mixtures were again incubated for 4 h prior to addition of 150 µl DMSO to dissolve the formed purple formazan crystals. The absorbance was measured after 1 h at 570 nm and 620 nm using Spectramax Multiplate reader (Molecular Devices, USA).

#### ***ii. Nuclear staining assay***

Different breast cancer cell lines (MDA MB 231 cell, 4T1 cells, and A431) were seeded in a 12 well tissue culture plate (50000 cells/well). After 24 h, the cells were treated with various concentrations of all four grades of TIONPs and incubated in 5% CO<sub>2</sub> at 37 °C for 24 h. After incubation, the cells were washed using PBS 7.4, fixed using 4% paraformaldehyde (500 µl/well) and stained using DAPI (10 µg/ml, 90 µl/well) and AO (100 µg/ml, 90 µl/well).

These plates were observed under fluorescence microscope at blue channel (358 nm) and green channel (480-490 nm) for DAPI and AO respectively.

### ***3.2.2. Development of doxorubicin loaded superparamagnetic IONPs for targeted drug delivery using external magnet (Work in progress)***

#### ***3.2.2.1. Preparation of doxorubicin loaded PVA coated superparamagnetic IONPs***

For this process, formulated bare IONPs with a definite concentration (0.5- 1 g) will be dispersed in freshly prepared PVA suspension and will be placed in stirrer for 12-24 h for achieving complete coating on the surface. 10 mg of doxorubicin will be mixed with 10 mL acetone and continuously stirred for 15-20 min to achieve uniform dispersion. The drug solution will be added drop wise to the colloidal solution of IONPs and stirred it for 6 h. Thereafter, the doxorubicin fabricated IONPs (Dox-IONPs) will be collected by eliminating the untrapped drug molecules using centrifugation followed by washing and drying in hot air oven [9]. All analytical characterization will be done to evaluate the formulated Dox-IONPs.

#### ***3.2.2.2. In-vitro drug release study***

For drug release study, Dox-TIONPs will be packed into the dialysis membrane and immersed in buffer solution with mild stirring. The samples will then be withdrawn with a regular time interval by replacing with freshly prepared buffer solutions. The absorbance of the collected samples will be measured using a UV-Vis spectrophotometer to calculate the percentage of drug release using a calibration curve of the standard drug solution [10].

#### ***3.2.2.3. In-vivo tumor volume reduction assay using externally guided magnet for targeted drug delivery***

##### ***i. Induction of tumor***

The in-vivo anticancer efficacy will be estimated through 4T1-Luc tumour-bearing mouse model using female balb-c mice. The animals will be kept in the institutional animal house following institutional animal ethical committee guidelines. The protocols will be approved by the committee beforehand. The 4T1-Luc cell suspension ( $1 \times 10^6$  cells/ 0.1 mL cell culture media) will be inoculated into the mammary fat pad of the mice to induce malignant tumor. The mice will be observed for about 10-14 days for tumor development [1]. After tumor development to a particular size/volume, animals will be randomized as mentioned below:

Group 1- Drug fabricated IONPs (Dox-IONPs) without external magnetic field treated

Group 2- Drug fabricated IONPs (Dox-IONPs) regulated by external magnetic field

Group 3- Control/ Saline

Group 4- Free Doxorubicin

The animals will be treated intravenously with desirable sample solutions when the tumor volume reaches 50- 100 mm<sup>3</sup>. The tumor volume will be calculated as follows:

$$V = 0.5 \times \text{longest diameter} \times (\text{shortest diameter})$$

#### ***ii. Anticancer efficacy by tumor volume reduction assay***

The treatment will be carried out with free Doxorubicin or Dox-IONPs. For group 2, a neodymium-boron-iron permanent magnet with a maximum flux density and 5mm diameter will be used to produce an inhomogeneous magnetic field for in vivo experiments. The magnet will be focused on the tumor during nanoparticle injection and will be maintained for 1 h post-injection. The tumor volume and body weight will be measured on every 2 days for all tumor bearing mice. After about 21 days of treatment, when the animals' tumor (control group) volumes reach 1000 mm<sup>3</sup>, the animals will be anesthetized under ketamine-xylazine, and the tumors will be collected by surgery and mice will be sacrificed for histopathological study.

#### ***iii. Immunohistochemistry analysis***

After sacrificing the animals, the selected organs (liver, kidney, heart, lung) will be subjected to histopathological study using Harris's hematoxylin- eosin (H & E) reagent. The morphological changes will be examined by light microscope to evaluate biocompatibility and biodistribution of the formulation.

### **4. Results and discussions**

#### ***4.1. Development and establishment of cytotoxic potential of IONPs from triphala extract using green synthesis technique***

##### ***4.1.1. Phytochemical analysis/ Identification of bioactive constituents***

The consumption of phenolic rich foods can minimize the risk factors associated with various types of cancers [29]. In a study with some traditional medicinal plants, Cai et al. (2004) established a positive correlation between antioxidant and total phenolic content with anticancer activity. They revealed significant chemo-preventive potency of traditional plants having strong antioxidant by virtue of their high phenolic content [30]. It is hypothesized that the phenolic compounds can strike the antioxidant levels with applicable in preventing cancer growing cells [31]. Apart from their potential in antioxidant and anticancer activity, phenols



and flavonoids can also act as reducing and capping agent for the biocompatible synthesis of nanoparticles [32].

Phenolic compounds, including flavonoids were found to be present in Triphala churna and its all three fruit ingredients. The total phenolic content was estimated using the gallic acid calibration curve  $y=0.0017x + 0.0259$  ( $R^2 = 0.9986$ ). It was found that the total phenolic content of Amlaki was maximum ( $198.85 \pm 0.02$  GAE/g), followed by Triphala churna, Bibhitaki, and Haritaki with values  $67.27 \pm 0.08$  GAE/g,  $55.90 \pm 0.02$  GAE/g, and  $39.17 \pm 0.05$  GAE/g respectively. Similarly, the total flavonoid content was calculated using Quercetin linear curve:  $y = 0.0024x + 0.0075$  ( $R^2 = 0.9997$ ). The total flavonoid content was seen to be maximum in aqueous extract of Bibhitaki ( $22.11 \pm 0.03$  mg Q/g) followed by Haritaki ( $12.09 \pm 0.01$  mg Q/g), Triphala churna ( $7.10 \pm 0.01$  mg Q/g), and Amlaki ( $5.48 \pm 0.03$  mg Q/g). The high phenolic and flavonoid content of Triphala churna, therefore, justifies their utilization in the green synthesis of IONPs for anticancer therapy.

HPTLC, an advanced chromatographic technique having high resolution power, is used to identify the visualizing spots for major active phytoconstituents present in natural products. It can be used as an excellent tool for quality control and standardization of any type of herbal formulation to identify each and every individual ingredients present in an herbal formulation [24].

HPTLC chromatographic 3D fingerprinting analysis of aqueous Triphala extract along with individual ingredients was successfully carried out by CAMAG HPTLC system (Fig. 1) for qualitative standardisation of the Triphala churna formulation. The figure elucidates different visualizing spots on HPTLC silica plates via selected mobile phase at 254 nm, 366 nm and 540 nm. The  $R_f$  values of different constituents at 254 nm, 366 nm, and 540 nm (white visible light) are given in Table 1 which confirmed the presence of all the constituents in Triphala churna formulation. The major  $R_f$  value for Triphala churna was noticed at 0.88, 0.87, 0.60, 0.53, 0.77, 0.79, 0.72, 0.90 which are contributed from *Embellica officinalis* (0.88, 0.53), *Terminalia chebula* (0.87, 0.60, 0.79), and *Terminalia bellirica* (0.90, 0.77, 0.72).

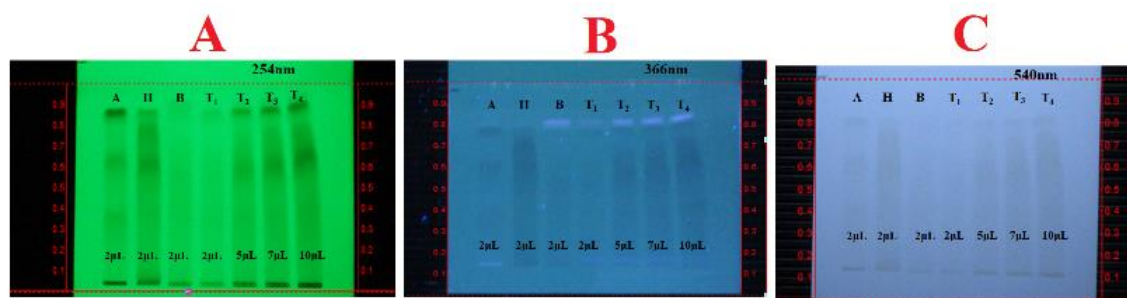


**Fig. 1.** HPTLC profile of Triphala Churna and its ingredients at (a) 254 nm (b) 366nm (c) 540nm [A. *Embellica officinalis* (Amlaki), H. *Terminalia chebula* (Haritaki) B. *Terminalia bellirica* (Bahera), T<sub>1</sub>- Triphala churna (2µL), T<sub>2</sub>- Triphala churna (5µL), T<sub>3</sub>- Triphala churna (7µL), T<sub>4</sub>- Triphala churna (10µL).

**Table 1: HPTLC analysis of individual extracts with Triphala churna extract**

R <sub>f</sub> Values						
Track 1 (A- <i>Embellica officinalis</i> )	Track 2 (H- <i>Terminalia chebula</i> )	Track 3 (B- <i>Terminalia bellirica</i> )	Track 4 (T <sub>1</sub> - Triphala churna 2µl)	Track 5 (T <sub>2</sub> - Triphala churna 5µl)	Track6 (T <sub>3</sub> - Triphala churna 7µl)	Track 7 (T <sub>4</sub> - Triphala churna 10µl)
0.88	0.87	0.90	0.86	0.87	0.88	0.90
0.65	0.79	0.84	0.84	0.76	0.79	0.94
0.60	0.60	0.72	0.58	0.60	0.72	0.87
0.53	0.56	0.77	0.81	0.53	0.60	0.77
0.37	0.35			0.36	0.64	0.72
					0.58	0.68

#### 4.1.2. Green synthesis and visual inspection of TIONPs

IONPs were prepared by green route using aqueous extract of Triphala churna and the reaction progress was observed through visualization mode. Fig. 2 represents the steps involved in the biosynthesis of TIONPs. The colour of the solution was changed from reddish-orange to lightish black instantly after the addition of churna extract to the iron salt solution which confirmed the reduction of Fe<sup>3+</sup> ions and subsequent formation of TIONPs.

During the process optimization, the maximum UV absorbance peak by the synthesized TIONPs was found at pH 11, indicating that the yield of the synthesized TIONPs is maximum in the alkaline medium. The colour was changed to deep black on stirring the reaction mixture for just 30 min, confirming the rapid formation of TIONPs within this brief reaction time. The % yield of the synthesized TIONPs was found to be 51.85 %.



**Fig. 2.** Steps involved in biosynthesis of TIONPs

#### **4.1.3. Characterization of TIONPs**

The UV-Visible spectral analysis was conducted to evaluate the absorption spectrum of formulated IONPs for initial confirmation of synthesis. The surface plasmon resonance peaks of TIONPs observed in the 260-280 nm regions were similar to the other reported studies with the IONPs with the maximum light absorption of TIONPs was recorded at 271 nm [33-37]. The comparative UV-Vis spectrophotometric scan of ferric chloride solution, Triphala churna extract, and the synthesized TIONPs solution are elucidated in Fig. 3a. The effect of pH and synthesis time on the yield of synthesized TIONPs are shown in Fig. 3b and Fig. 3c respectively. It is evident that the synthesis is favoured in alkaline medium. Moreover, reaction time of 30 min was enough for complete synthesis of iron oxide nanoparticles from the aqueous extract of Triphala churna. As per this observation, the optimum pH and synthesis time was set at 11 and 30 min respectively. The TIONPs thus formed were processed for further characterizations and evaluation of biological activities. Additionally, the AAS was used to determine the iron concentration present in the formulated nanoparticles (TIONPs) by the help of Ferrous chloride calibration curve ( $y = 0.0351x - 0.0006$ ,  $R^2 = 0.9977$ ). The total iron content in the sample was found to be 23.70 %.

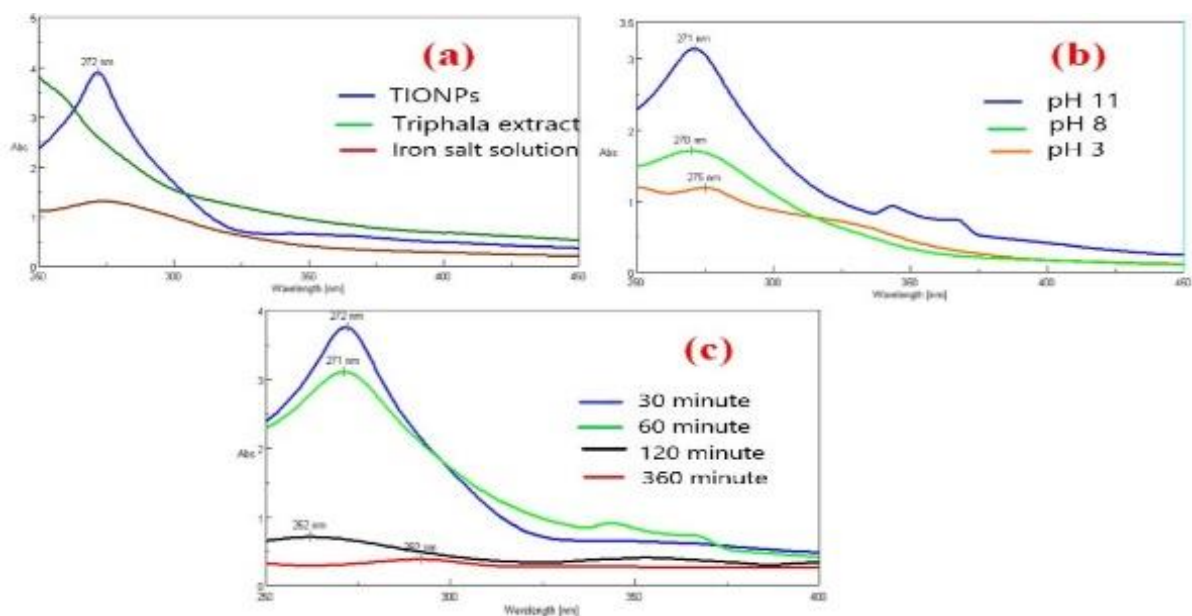


**Fig.3.** UV-Visible spectrophotometer of TIONPs (a) Spectrum of  $\text{FeCl}_3$  solution, triphala extract and TIONP suspension; (b) Comparative pH variant study; (c) Comparative time variant study

The FTIR analysis was conducted within  $400\text{--}4000\text{ cm}^{-1}$  to identify the functional groups responsible for stabilizing and capping of TIONPs. In the FT-IR spectrum (Fig. 4), the  $514.90\text{ cm}^{-1}$  peak is attributed to the stretching of Fe-O of  $\text{Fe}_2\text{O}_3$  or  $\text{Fe}_3\text{O}_4$  while the peak at  $1058.73\text{ cm}^{-1}$  is due to C-O stretching. Moreover, the peak at  $1195.65\text{ cm}^{-1}$  denotes the presence of Fe-OH group. The small peak around  $1430.92\text{ cm}^{-1}$  is due to the OH stretching and deformation by the water molecular vibration [36, 38]. The FT-IR results indicate that prepared IONPs are capped with biologic compounds derived from Triphala churna extract. Additionally, -OH bend of phenol are depicted by an intense peak at  $1329.68\text{ cm}^{-1}$  and -C=O peak at  $1712.5\text{ cm}^{-1}$  of formulated TIONPs. It also displayed a broad peak of N-H stretch at  $3198.36\text{ cm}^{-1}$ . FTIR analysis confirms the presence of amines, phenols, carbonyl, and alkene group that possess a strong binding affinity towards iron and significantly act as reducing and capping agent for the reduction of ferrous ions [39].

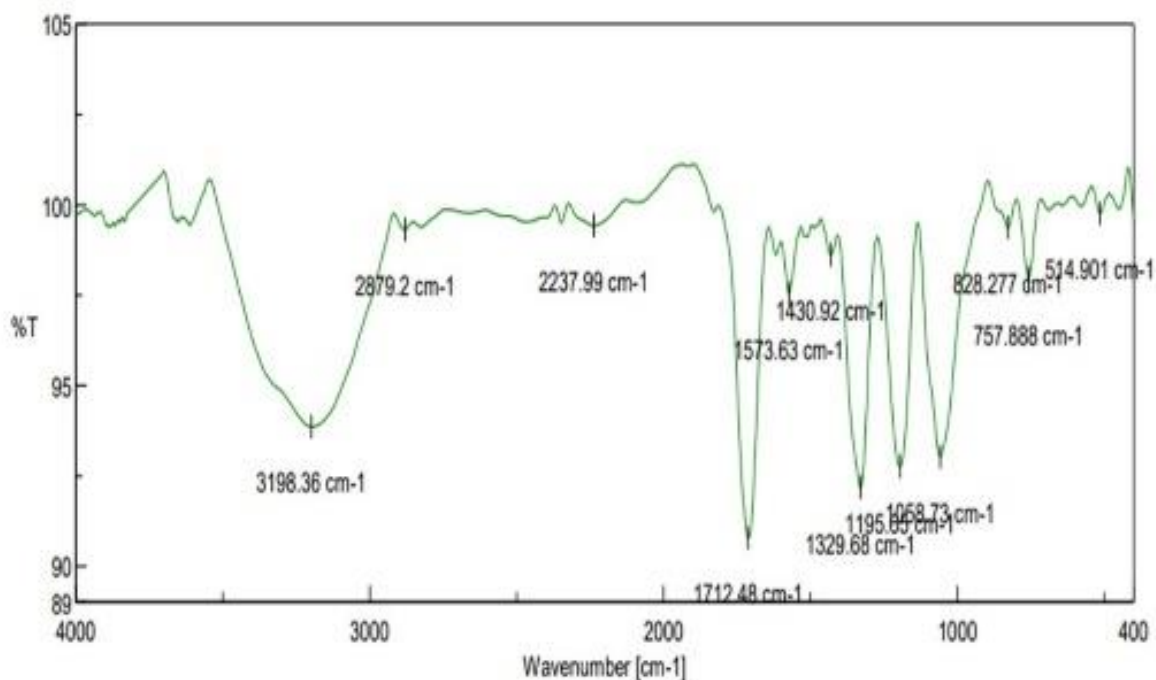


**Fig. 4.** FT-IR spectroscopy of TIONPs

X-ray Diffraction (XRD) is an important analytical tool for the examination of the crystalline phase of nanoparticles. The XRD pattern of TIONPs is provided in Fig. 5. The diffraction peaks of hematite nanoparticles ( $\alpha$ -Fe<sub>2</sub>O<sub>3</sub>) are exhibited at 23.38° and 69.72°, while the diffraction peaks at 27.06°, 38.70°, and 55.75° are indicative of the maghemite ( $\gamma$ -Fe<sub>2</sub>O<sub>3</sub>) nanoparticles [40]. The synthesized IONPs are therefore found to be a mixture of hematite and maghemite nanoparticles [41]. Some other small peaks were observed due to the endorsement of organic materials adsorbed from Triphala extract as capping agents.

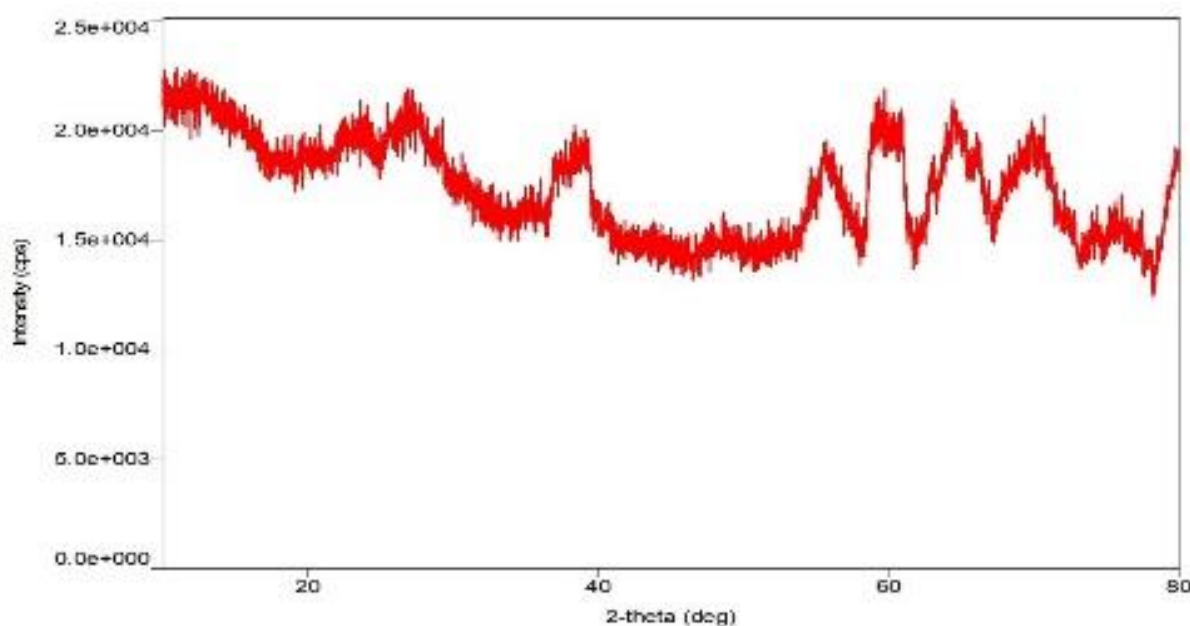


**Fig. 5.** X-Ray Diffraction pattern of synthesized TIONPs

The morphological structure of green synthesized TIONPs was examined by scanning electron microscope (SEM). The SEM images (Fig. 6) revealed that the synthesized iron oxide nanoparticles were spherical within the range of 29-74 nm. Zeta potential data represents the stability and electrostatic potential (attraction and repulsion of particles in suspension) of formulated nanoparticles. In our studies, the average particles size distribution and the zeta potential of the synthesized TIONPs measured by DLS- zeta sizer was recorded at -2.95 mV (Fig. 7). Due to the presence of this lower amount of charges on the surface of the TIONPs, there is possibility of agglomeration of nanoparticles. Although, it can be easily tackled by coating these nanoparticles with biocompatible polymer to enhance their stability prior to their utilization in biomedical fields like targeted drug delivery. Moreover, it is also previously reported that the similar low zeta potential can result in formation of stable nanoparticles [42]. The evaluation of hydrodynamic diameter, polydispersity index (PDI), and average particle size of TIONPs was also conducted by DLS (Fig. 7). The narrow size distribution in the range between 35 to 100 nm confirmed the good size reduction of the TIONPs. The intensity peak in the statistics curve revealed that the average particle size of TIONPs was around 167 nm which was suitable enough to cross the biological barriers effortlessly to target a specific site during drug delivery. The PDI value of 0.246 indicated the homogenous distribution of particles within the solution. It is reported that the nanoparticle PDI value lesser than 0.3 is acceptable for their drug delivery applications [43]. Thus, the results clearly demonstrated the monodispersive nature of our synthesized TIONPs.



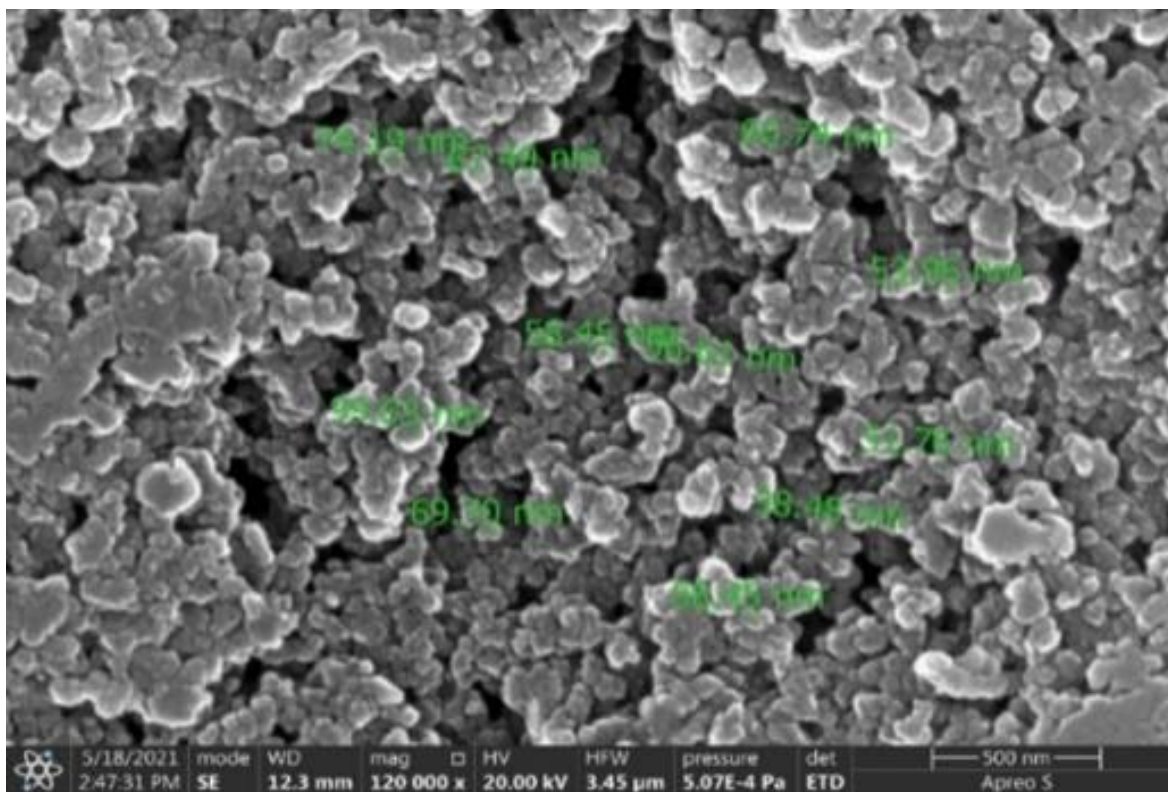


**Fig. 6.** SEM images of formulated TIONPs at scale bar of 500 nm

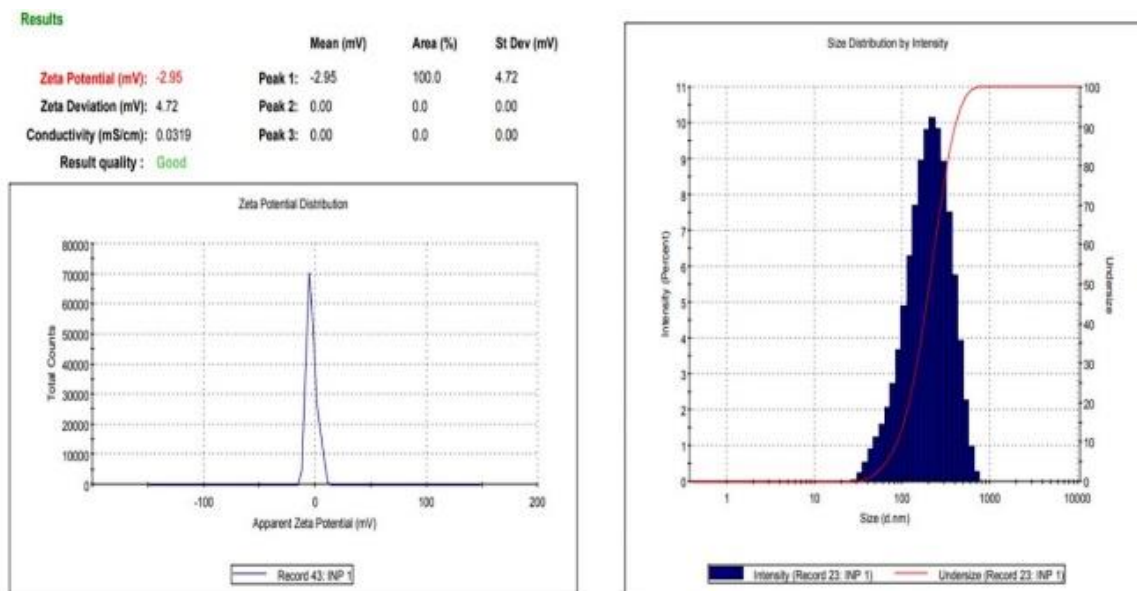


**Fig. 7.** DLS-Zeta potential analysis of synthesized TIONPs

The magnetic characterization of TIONPs was monitored at room temperature by SQUID-VSM magnetometer (Fig. 8). The results showed the linear M-H graph with no hysteresis loop, which confirmed the paramagnetic nature of synthesized TIONPs [44]. Paramagnetism is a kind of magnetic nature of materials that is weakly attracted by a strong externally applied magnetic field. This paramagnetic property may become helpful to regulate the movement of the TIONPS within body by a strong external magnetic field to facilitate their site specific action [45].

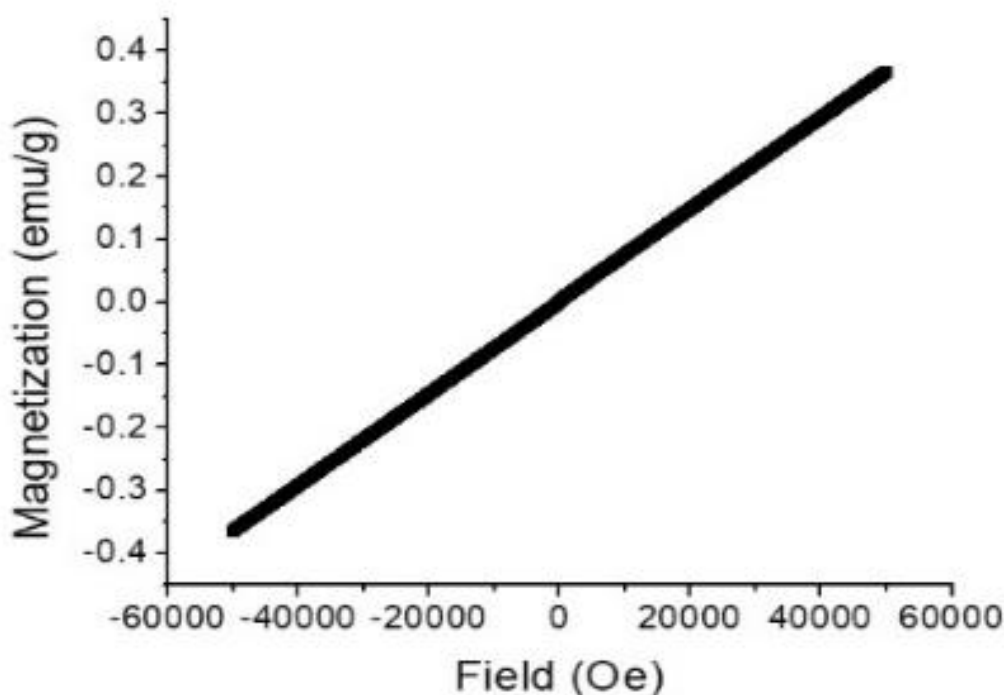


**Fig. 8.** Magnetic moment analysis of synthesized TIONPs by SQUID

#### **4.1.4. *In-Vitro Antioxidant and Anti-inflammatory assay***

The active metabolites present in the plant products can exert a wide range of biological activities. The phenolic and flavonoid-like constituents are mainly responsible for the scavenging of free radicals and break the chain of lipid oxidation reaction by phenolic hydroxyl groups [46]. The uncontrolled production of free radicals or reactive oxygen species (ROS) in the body leads for the abnormal epithelial cell growth and ultimately developing the breast cancer [47]. Hence, the antioxidant and anti-inflammatory activity of TIONPs was evaluated in support of their potential in the treatment of breast cancer.

The free radical scavenging activity was evaluated by performing the DPPH assay method using ascorbic acid as standard reference. The IC<sub>50</sub> value for ascorbic acid, Triphala extract



and TIONPs were 7.693, 5.666 and 20.280 ( $\mu\text{g/mL}$ ) respectively. The scavenging activity of aqueous extract of Triphala was found to be higher than that of the TIONPs due to the lower concentration of biomolecules in TIONPs suspension (Fig. 9A). Moreover, this observed free radical scavenging activity of TIONPs was found to be concentration dependent.

The in-vitro anti-inflammatory assay was done by protein denaturation method by using bovine serum albumin where diclofenac sodium as standard drug. The result revealed that the synthesised TIONPs were effective in inhibiting protein denaturation of albumin with 88.23% inhibition by the highest concentration (100  $\mu\text{g/mL}$ ) of the product (Fig. 9B). Interestingly, the TIONPs showed a better and significant anti-inflammatory activity than Triphala churna extract advocating the advantage of administering this nano formulation over the conventional Ayurvedic churna. Our TIONPs having inherent antioxidant and anti-inflammatory activity is thus expected to stabilize and control the formation of excess free radicals to reduce the abnormal proliferation of breast cancer cells.

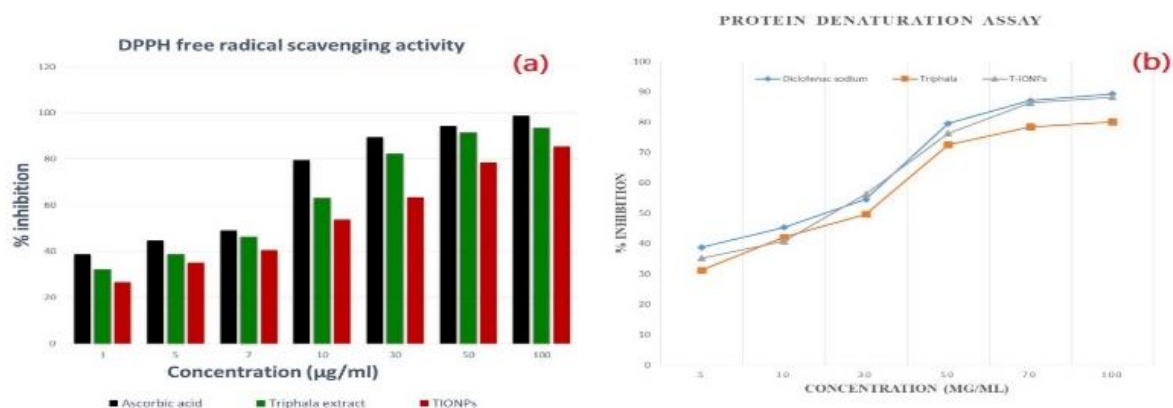


**Fig. 10.** Free radical scavenging activity of TIONPs by DPPH assay (a) In-vitro anti-inflammatory activity of TIONPs by protein denaturation assay (b)

#### 4.1.5. MTT assay

The secondary breast cancer leads to metastasis of skin due to the rapid growth of cancerous cells towards subcutaneous or squamous cell. From a case study, it was elucidated that the breast cancer can lead to skin cancer through skin of chest, scalp, neck, and abdomen or through the blood capillaries or lymphatic system [48]. Thus, in this research work the cytotoxic effect and efficacy of synthesized TIONPs was evaluated in two TNBC specific cell lines namely, MDA MB231 and 4T1, along with a skin cancer cell line (A431). A healthy cell line (HEK 293) was kept as control to assess the treatment selectivity and safety towards normal cells.

The MTT cell viability assay indicates the percentage of healthy and live cells in a sample to quantify the rate of live and dead cell or cell proliferation. It is a type of colorimetric assay which is used to quantify the number of metabolically active cells with the intensity of the colour produced. In general, the cell viability of cancerous cell in the MTT assay, should be less than that of control normal cell to ensure the cytotoxic effect of the anticancer drug[49]. In our study, the TIONPs sample showed lesser percentage of live cancerous cells in comparison to the control cell (HEK 293) which implies the cytotoxic potential of TIONPs towards TNBC and A431 cell. The test results are represented in Fig. 10 where the anticancer efficacy of Triphala churna mediated IONPs was expressed in terms of the concentration causing 50% decrease in cell viability ( $IC_{50}$ ,  $\mu\text{g/mL}$ ). For MDA MB 231 cell lines, TIONPs showed % cell viability of  $38.56 \pm 4.53$  and  $35.56 \pm 2.53$  at concentration of  $500 \mu\text{g/mL}$  in 24 h and 48 h respectively. For 4T1 cell lines it showed % cell viability of  $35 \pm 1.41$  and  $25.42 \pm 1.84$  at concentration  $500 \mu\text{g/mL}$  in 24 h and 48 h respectively. They also exerted  $32 \pm 1.47$  % cell viability at the  $500 \mu\text{g/mL}$  concentration in 24 h and  $25.24 \pm 2.14$  % cell viability in 48 h for A431 cell lines. However, the non-cancerous (HEK) cell line showed much higher cell viability of  $72 \pm 1.58$  % and  $54.30 \pm 1.25$  % respectively at  $500 \mu\text{g/mL}$  concentrations in 24 h and 48 h.

For both breast cancer (4T1, MDA MB 231) and skin cancer cell line (A431), a cell viability investigation revealed that the formulation (TIONPs) promoted greater cellular internalization and resulted in lower cell viability, indicating the cytotoxic nature of synthesized TIONPs towards cancer cell. The data also revealed that the said activity was concentration and time-dependant as the % of cell viability was gradually decreased with both concentration and time. The TIONPs were found to exert much less cytotoxic effect against the normal (host) cells in comparison to the cancerous cells, which advocate their use as potent anticancer agents in the future. Additionally, it is already observed that the IONPs are considered to be safe and nontoxic for human consumption as iron is a naturally occurring mineral in human body [50].

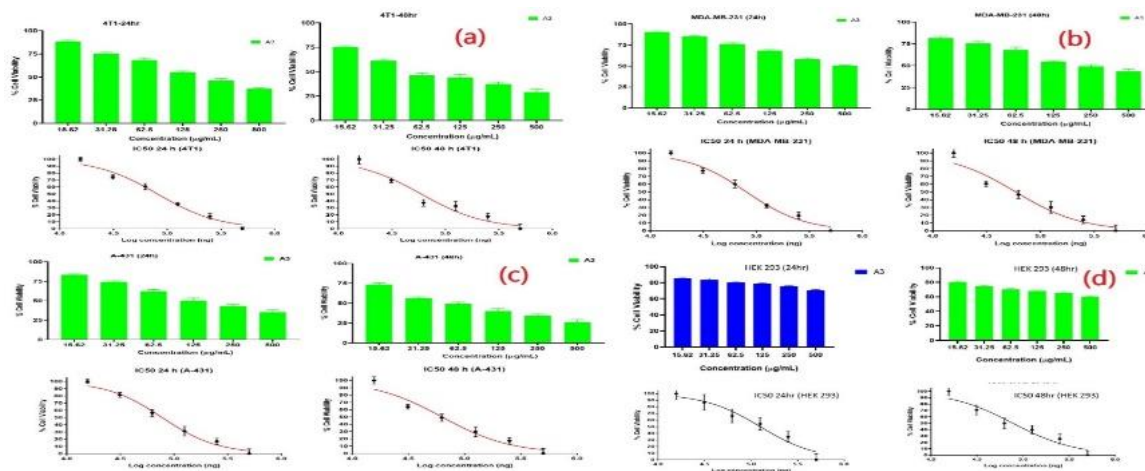


**Fig. 11.** In vitro cytotoxicity study of TIONPs (a) Cell viability study and IC<sub>50</sub> value of 4T1 cells after treatment for 24 h and 48h (b) Cell viability study and IC<sub>50</sub> value of MDA MB231 cells after treatment for 24 h and 48h (c) Cell viability study and IC<sub>50</sub> value of A431 cells after treatment for 24 h and 48h (d) Cell viability study and IC<sub>50</sub> value of HEK 293cells after treatment for 24 h and 48h of HEK 293cells

#### 4.1.6. Nuclear Staining Assay

The nuclear staining assay is used as a support to MTT assay to investigate whether the test sample mediated cell death is induced by apoptosis or necrosis. The apoptosis indicates the programmed cell death without disturbing the normal function of the body. While, thenecrosis is considered as the alternative to apoptosis where inappropriate or accidental cell death occurs by means of a toxic process. Thus, apoptosis is more preferable during cytotoxicity activity than necrosis to avoid the negative circumstances of immune system. The occurrence of apoptosis can be measured by nuclear staining assay by observing the morphological hallmarks like nucleus breakdown, collapsed chromatin fragmentation, nuclear envelope destruction and cell blebbing [51]. In our studies, the apoptotic cell population were observed by staining the nucleus using DAPI and AO after treatment with TIONPs. From the result it was confirmed that synthesized nanoparticles (TIONPs) induced maximum chromatin condensation, cell blebbing and cell shrinkage for MDA MB 231 cell lines. In case of the 4T1 and A431 cell lines, TIONPs treated cells induced more nuclear fragmentation and cytoplasmic shrinkage. AO penetrated both normal and dead cell and generated green fluorescence. Our study indicates that the viable cells show green fluorescence and the normal cell characteristic of uniform chromatin with an intact cell membrane, whereas, nuclear fragmentation and membrane bubbles represents early apoptosis (Fig. 11). The late apoptosis cells exhibited white nuclei with condensed or fragmented chromatin. The results

represented that the synthesized compound induced the majority of cell death through apoptosis mode indicating potent anticancer activity of TIONPs.

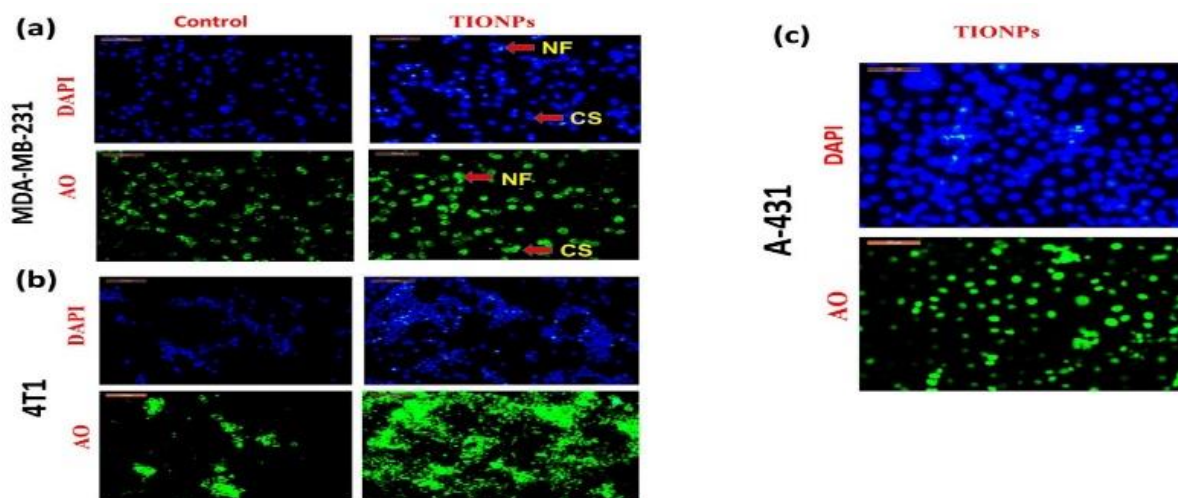


**Fig. 12.** Nuclear staining assay of TIONPs (a) MDA-MB-231 (b) 4T1 (c) A-431 cell lines

#### ***4.2. Development of doxorubicin loaded superparamagnetic IONPs for targeted drug delivery using external magnet (Continuing work)***

##### **Work progress and expected outcomes**

The optimised IONPs have already been synthesized employing green chemistry techniques, and the results demonstrated the superparamagnetic nature of IONPs, which could be helpful in targeted drug delivery applications. The samples have already been sent for other analytical characterizations. The work progression for this strategy is shown in Fig. 13. The next strategy will just focus on the tumour induction and in-vivo tumour volume reduction assay for targeted drug administration using an external magnetic field.

If this proof of principle is successfully established, the product(s) is/are expected to be well regulated by external magnetic field to facilitate targeted drug delivery of anticancer/poorly bioavailable drugs for their better efficacy and lesser systemic toxicity. I shall also attempt for patenting our technology/product. Additionally, we shall reach out to relevant stakeholders for clinical trial and subsequent commercialization of our developed product(s).

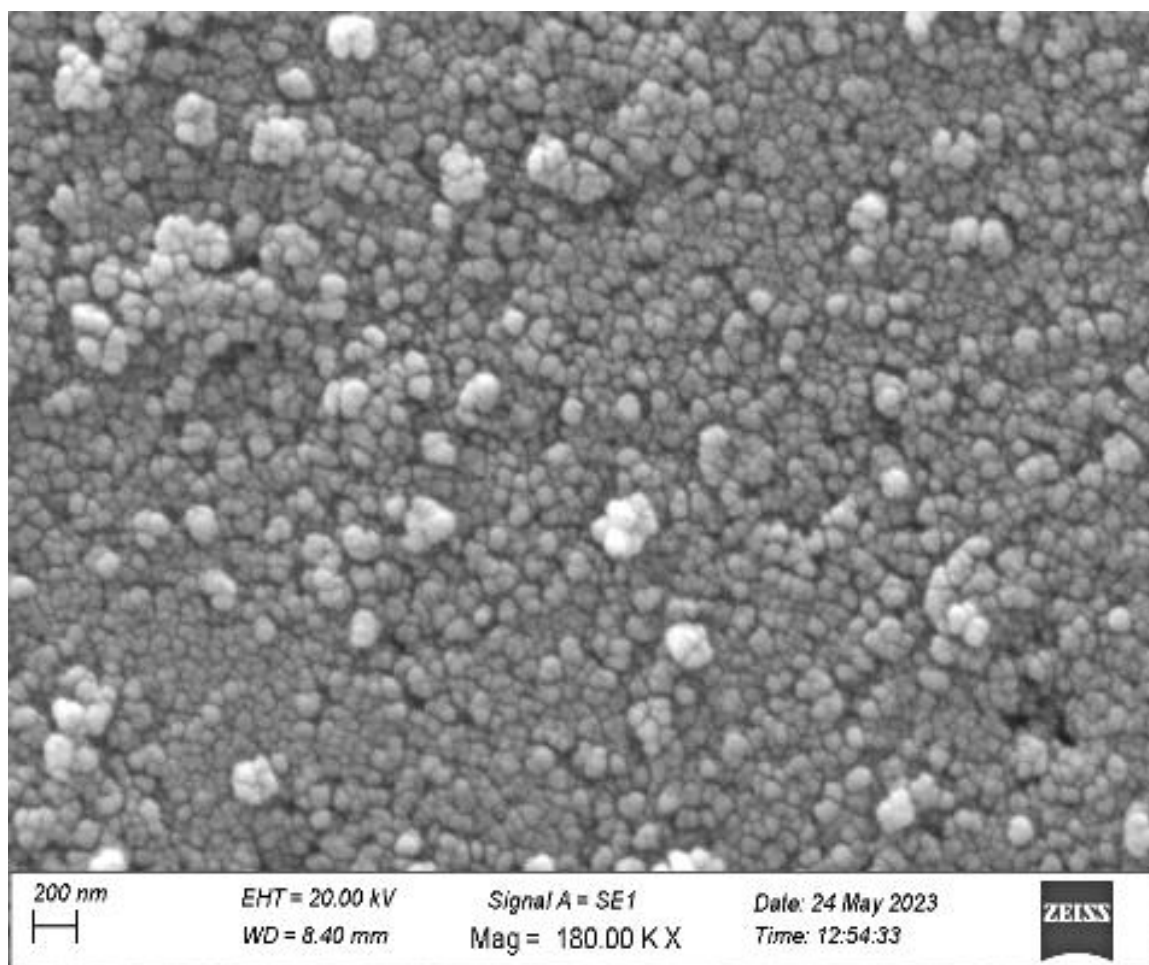


Fig 13. SEM images of Superparamagnetic IONPs

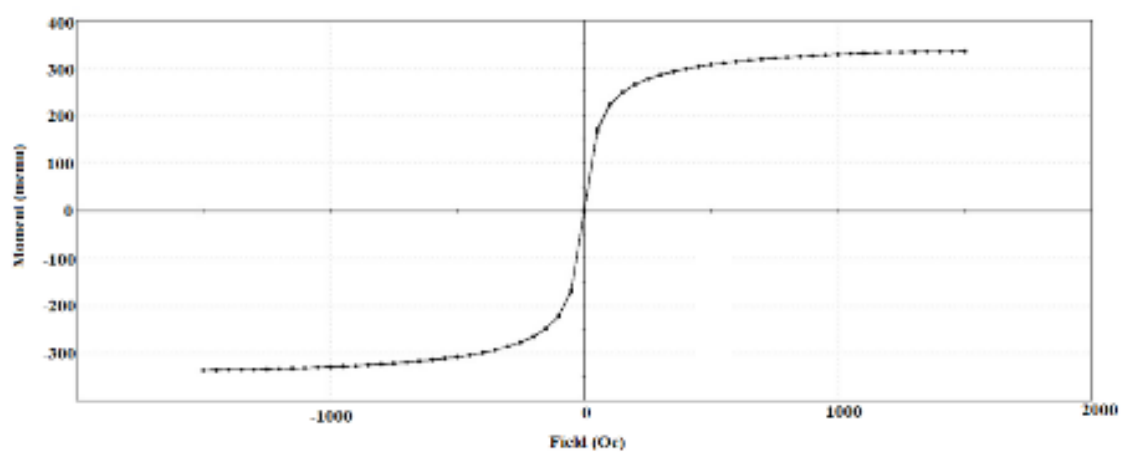


Fig.14. VSM of Superparamagnetic IONPs

## **5. Impact of the research in the advancement of knowledge or benefit to mankind**

- Diagnosis and treatment of breast cancer is a challenging task. Free chemotherapeutic drugs used to treat cancer have serious drawbacks such as dose limitation, poor bioavailability, and high price resulting severe systemic side effects with huge financial burden for the patients of low and medium income countries.
- Superparamagnetic IONPs can be a great option to the above said problem as it smoothly carry the drug at the targeted site without causing any harm to the normal cells by the help of an external strong magnet.
- Our developed superparamagnetic IONPs will attempt to minimize the treatment limitations through external magnetic field guided accumulation of drug selectively at the targeted breast cancer cell site and thereby reducing its administered daily dose for improved safety and efficacy. Additionally, the biodistribution and toxicity assessment will be done to confirm the reduction in risk of accumulation of drug at any other site of body and its associated toxicity.
- After the establishment of successful pre-clinical and clinical trials, our developed superparamagnetic IONPs can be sold as a parenteral product for the external magnet therapy of breast cancer. This kind of medicine should be launched as quickly as possible to help many people overcome this difficulty, as breast cancer is a serious concern now across the globe. Although the marketability of this sort of product (superparamagnetic IONPs) is enormous, no product for the treatment of breast cancer has yet been commercialised.
- SUN pharma is regarded as a top most leading pharmaceutical company where all variety of products are available.

## **6. Literature references**

- [1] Huang L, Weng X, Chen Z, Megharaj M, Naidu R. Green synthesis of iron nanoparticles by various tea extracts: comparative study of the reactivity. *Spectrochimica Acta Part A: Molecular and Biomolecular Spectroscopy*. 2014 Sep 15;130:295-301. <https://doi.org/10.1016/j.saa.2014.04.037>
- [2] Wilkinson L, Gathani T. Understanding breast cancer as a global health concern. *The British Journal of Radiology*. 2022 Feb 1;95(1130):20211033. <https://doi.org/10.1259/bjr.20211033>
- [3] de Ruijter TC, Veeck J, de Hoon JP, van Engeland M, Tjan-Heijnen VC. Characteristics of triple-negative breast cancer. *Journal of cancer research and clinical oncology*. 2011 Feb;137(2):183-92. <https://doi.org/10.3389/fonc.2021.710337>
- [4] Shaikh SS, Emens LA. Current and emerging biologic therapies for triple negative breast cancer. *Expert Opinion on Biological Therapy*. 2022 May 4;22(5):591-602. <https://doi.org/10.1080/14712598.2020.1801627>



- [5] Chowdhury P, Ghosh U, Samanta K, Jaggi M, Chauhan SC, Yallapu MM. Bioactive nanotherapeutic trends to combat triple negative breast cancer. *Bioactive Materials*. 2021 Oct 1;6(10):3269-87. <https://doi.org/10.1016/j.bioactmat.2021.02.037>
- [6] Yadwade R, Kirtiwar S, Ankamwar B. A review on green synthesis and applications of iron oxide nanoparticles. *Journal of Nanoscience and Nanotechnology*. 2021 Dec 1;21(12):5812-34.<https://doi.org/10.1166/jnn.2021.19285>
- [7] Jiang K, Zhang L, Bao G. Magnetic iron oxide nanoparticles for biomedical applications. *Current Opinion in Biomedical Engineering*. 2021 Dec 1;20:100330. <https://doi.org/10.1016/j.cobme.2021.100330>
- [8] World Health Organization. Cancer Control: Knowledge Into Action: WHO Guide for Effective Programmes. Policy and Advocacy. Module 6. World Health Organization; 2008.
- [9] Thakor AS, Gambhir SS. Nanooncology: the future of cancer diagnosis and therapy. *CA: a cancer journal for clinicians*. 2013 Nov;63(6):395-418. <https://doi.org/10.3322/caac.21199>
- [10] Bilia AR, Bergonzi MC. The G115 standardized ginseng extract: An example for safety, efficacy, and quality of an herbal medicine. *Journal of Ginseng Research*. 2020 Mar 1;44(2):179-93.<https://doi.org/10.1016/j.jgr.2019.06.003>
- [11] Ong ES. Extraction methods and chemical standardization of botanicals and herbal preparations. *Journal of Chromatography B*. 2004 Dec 5;812(1-2):23-33. <https://doi.org/10.1016/j.jchromb.2004.07.041>
- [12] Shivakumar A, Paramashivaiah S, Anjaneya RS, Hussain J, Ramachandran S. Pharmacognostic evaluation of triphala herbs and establishment of chemical stability of triphala caplets. *Int J Pharm Sci Res*. 2016 Jan 1;7(1):244-51.
- [13] Kumar NS, Nair AS, Murali M, PS SD. Qualitative phytochemical analysis of triphala extracts. *Journal of Pharmacognosy and Phytochemistry*. 2017;6(3):248-51.
- [14] Kadam DK, Ahire PD, Bhoje JV, Patil AR, Yadav DK. Comparative standardization study of three Triphala churna formulation. *Int J Pharmacogn (Panchkula, India)*[Online]. 2018;4(2):71-8. [http://dx.doi.org/10.13040/IJPSR.0975-8232.IJP.3\(11\).482-90](http://dx.doi.org/10.13040/IJPSR.0975-8232.IJP.3(11).482-90)
- [15] Ahmed S, Ding X, Sharma A. Exploring scientific validation of Triphala Rasayana in ayurveda as a source of rejuvenation for contemporary healthcare: An update. *Journal of Ethnopharmacology*. 2021 Jun 12;273:113829. <https://doi.org/10.1016/j.jep.2021.113829>
- [16] Sandhya T, Lathika KM, Pandey BN, Mishra KP. Potential of traditional ayurvedic formulation, Triphala, as a novel anticancer drug. *Cancer letters*. 2006 Jan 18;231(2):206-14. <https://doi.org/10.1016/j.canlet.2005.01.035>
- [17] Cheriyaundath S, Mahaddalkar T, Save SN, Choudhary S, Hosur RV, Lopus M. Aqueous extract of Triphala inhibits cancer cell proliferation through perturbation of microtubule assembly dynamics. *Biomedicine & Pharmacotherapy*. 2018 Feb 1;98:76-81. <https://doi.org/10.1016/j.biopha.2017.12.022>
- [18] Prasad S, Srivastava SK. Oxidative stress and cancer: chemopreventive and therapeutic role of triphala. *Antioxidants*. 2020 Jan;9(1):72. <https://doi.org/10.3390/antiox9010072>
- [19] Murthy MS. Anticancer and pro-apoptotic effects of Triphala extract in human breast cancer MCF-7 cells. *The FASEB Journal*. 2018 Apr;32:151-2. [https://doi.org/10.1096/fasebj.2018.32.1\\_supplement.151.2](https://doi.org/10.1096/fasebj.2018.32.1_supplement.151.2)
- [20] Chakrapany S, Chandan S. Nano carriers of novel drug delivery system for 'ayurveda herbal remedies' need of hour—a bird's eye view. *American Journal of PharmTech Research*. 2014;4(2):60-9.

- [21] Ranjani S, Hemalatha S. Triphala decorated multipotent green nanoparticles and its applications. *Materials Letters*. 2022 Feb 1;308:131184. <https://doi.org/10.1016/j.matlet.2021.131184>
- [22] Jayajothi E, Elavarasu T, Hamsaveni M, Sridhar SK. Antioxidant activity and total phenolic content of triphala churna. *Natural Product Sciences*. 2004;10(1):16-9
- [23] Khorasani Esmaeili A, Mat Taha R, Mohajer S, Banisalam B. Antioxidant activity and total phenolic and flavonoid content of various solvent extracts from in vivo and in vitro grown *Trifolium pratense* L.(Red Clover). *BioMed Research International*. 2015 Oct;2015. <https://doi.org/10.1155/2015/643285>
- [24] Mukhi S, Bose A, Ray A, Swain PK. Analytical Standards of Amrtadi Churna: A Classical Ayurvedic Formulation. *Indian Journal of Pharmaceutical Sciences*. 2017 May 15;79(2):227-40. <https://doi.org/10.4172/pharmaceutical-sciences.1000221>
- [25] Sood R, Chopra DS. Improved yield of green synthesized crystalline silver nanoparticles with potential antioxidant activity. *Int. Res. J. Pharm*. 2017;8(4):100-4. <https://doi.org/10.7897/2230-8407.080457>
- [26] Prasad AS. Iron oxide nanoparticles synthesized by controlled bio-precipitation using leaf extract of Garlic Vine (*Mansoa alliacea*). *Materials Science in Semiconductor Processing*. 2016 Oct 1;53:79-83. <http://dx.doi.org/10.1016/j.mssp.2016.06.009>
- [27] Abdullah JA, Eddine LS, Abderrhmane B, Alonso-González M, Guerrero A, Romero A. Green synthesis and characterization of iron oxide nanoparticles by pheonix dactylifera leaf extract and evaluation of their antioxidant activity. *Sustainable Chemistry and Pharmacy*. 2020 Sep 1;17:100280. <https://doi.org/10.1016/j.scp.2020.100280>
- [28] Gunathilake KD, Ranaweera KK, Rupasinghe HP. In vitro anti-inflammatory properties of selected green leafy vegetables. *Biomedicines*. 2018 Dec;6(4):107. <https://doi.org/10.3390/biomedicines6040107>
- [29] Anantharaju PG, Gowda PC, Vimalambike MG, Madhunapantula SV. An overview on the role of dietary phenolics for the treatment of cancers. *Nutrition journal*. 2016 Dec;15(1):1-6. <https://doi.org/10.1186/s12937-016-0217-2>
- [30] Cai Y, Luo Q, Sun M, Corke H. Antioxidant activity and phenolic compounds of 112 traditional Chinese medicinal plants associated with anticancer. *Life sciences*. 2004 Mar 12;74(17):2157-84. <https://doi.org/10.1016/j.lfs.2003.09.047>
- [31] Sakakibara H, Honda Y, Nakagawa S, Ashida H, Kanazawa K. Simultaneous determination of all polyphenols in vegetables, fruits, and teas. *Journal of agricultural and food chemistry*. 2003 Jan 29;51(3):571-81 <https://doi.org/10.1021/jf020926l>
- [32] Alegria EC, Ribeiro AP, Mendes M, Ferraria AM, Do Rego AM, Pombeiro AJ. Effect of phenolic compounds on the synthesis of gold nanoparticles and its catalytic activity in the reduction of nitro compounds. *Nanomaterials*. 2018 May;8(5):320. <https://doi.org/10.3390/nano8050320>
- [33] Pillai RR, Sreelekshmi PB, Meera AP, Thomas S. Biosynthesized iron oxide nanoparticles: Cytotoxic evaluation against human colorectal cancer cell lines. *Materials Today: Proceedings*. 2022 Jan 20. <https://doi.org/10.1016/j.matpr.2022.01.151>
- [34] Demirezen DA, Yıldız YŞ, Yılmaz Ş, Yılmaz DD. Green synthesis and characterization of iron oxide nanoparticles using *Ficus carica* (common fig) dried fruit extract. *Journal of bioscience and bioengineering*. 2019 Feb 1;127(2):241-5. <https://doi.org/10.1016/j.jbiosc.2018.07.024>
- [35] Katata-Seru L, Moremedi T, Aremu OS, Bahadur I. Green synthesis of iron nanoparticles using *Moringa oleifera* extracts and their applications: removal of nitrate from water and antibacterial activity against *Escherichia coli*. *Journal of Molecular Liquids*. 2018 Apr 15;256:296-304. <https://doi.org/10.1016/j.molliq.2017.11.093>



- [36] Bhuiyan MS, Miah MY, Paul SC, Aka TD, Saha O, Rahaman MM, Sharif MJ, Habiba O, Ashaduzzaman M. Green synthesis of iron oxide nanoparticle using Carica papaya leaf extract: application for photocatalytic degradation of remazol yellow RR dye and antibacterial activity. *Heliyon*. 2020 Aug 1;6(8):e04603. <https://doi.org/10.1016/j.heliyon.2020.e04603>
- [37] Ali HR, Nassar HN, El-Gendy NS. Green synthesis of  $\alpha$ -Fe<sub>2</sub>O<sub>3</sub> using Citrus reticulum peels extract and water decontamination from different organic pollutants. *Energy Sources, Part A: Recovery, Utilization, and Environmental Effects*. 2017 Jul 3;39(13):1425-34. <https://doi.org/10.1080/15567036.2017.1336818>
- [38] Arularasu MV, Devakumar J, Rajendran TV. An innovative approach for green synthesis of iron oxide nanoparticles: Characterization and its photocatalytic activity. *Polyhedron*. 2018 Dec 1;156:279-90. <https://doi.org/10.1016/j.poly.2018.09.036>
- [39] Gangopadhyay, A., Saha, R., Bose, A., Sahoo, R.N., Nandi, S., Swain, R., Paul, M., Biswas, S. and Mohapatra, R., 2022. Effect of annealing time on the applicability of potato starch as an excipient for the fast disintegrating propranolol hydrochloride tablet. *Journal of Drug Delivery Science and Technology*, 67, p.103002. <https://doi.org/10.1016/j.jddst.2021.103002>
- [40] Cheng Z, Tan AL, Tao Y, Shan D, Ting KE, Yin XJ. Synthesis and characterization of iron oxide nanoparticles and applications in the removal of heavy metals from industrial wastewater. *International Journal of Photoenergy*. 2012 May;2012. <https://doi.org/10.1155/2012/608298>
- [41] Devi HS, Boda MA, Shah MA, Parveen S, Wani AH. Green synthesis of iron oxide nanoparticles using Platanus orientalis leaf extract for antifungal activity. *Green Processing and Synthesis*. 2019 Jan 1;8(1):38-45. <https://doi.org/10.1515/gps-2017-0145>
- [42] Singh M, Kaur R, Rajput R, Agarwal S, Kumar S, Sharma M, Sharma A. Analysis of Process and Formulation Variables on Chitosan based Losartan Potassium Nanoparticles: Preparation, Validation and in vitro Release Kinetics. *Recent Innovations in Chemical Engineering (Formerly Recent Patents on Chemical Engineering)*. 2020 Feb 1;13(1):41-54
- [43] Danaei M, Dehghankhold M, Ataei S, Hasanzadeh Davarani F, Javanmard R, Dokhani A, Khorasani S, Mozafari MR. Impact of particle size and polydispersity index on the clinical applications of lipidic nanocarrier systems. *Pharmaceutics*. 2018 May 18;10(2):57
- [44] Ardakani LS, Alimardani V, Tamaddon AM, Amani AM, Taghizadeh S. Green synthesis of iron-based nanoparticles using Chlorophytum comosum leaf extract: Methyl orange dye degradation and antimicrobial properties. *Heliyon*. 2021 Feb 1;7(2):e06159. <https://doi.org/10.1016/j.heliyon.2021.e06159>
- [45] Beheshtkhoo N, Kouhbanani MA, Savardashtaki A, Amani AM, Taghizadeh S. Green synthesis of iron oxide nanoparticles by aqueous leaf extract of Daphne mezereum as a novel dye removing material. *Applied Physics A*. 2018 May;124(5):1-7. <https://link.springer.com/article/10.1007%2Fs00339-018-1782-3>
- [46] Choudhury B, Kandimalla R, Elancheran R, Bharali R, Kotoky J. Garcinia morella fruit, a promising source of antioxidant and anti-inflammatory agents induces breast cancer cell death via triggering apoptotic pathway. *Biomedicine & Pharmacotherapy*. 2018 Jul 1;103:562-73. <https://doi.org/10.1016/j.biopha.2018.04.068>
- [47] Reuter S, Gupta SC, Chaturvedi MM, Aggarwal BB. Oxidative stress, inflammation, and cancer: how are they linked?. *Free radical biology and medicine*. 2010 Dec 1;49(11):1603-16. <https://dx.doi.org/10.1016%2Fj.freeradbiomed.2010.09.006>
- [48] Adams S, Kozhaya L, Martiniuk F, Meng TC, Chiriboga L, Liebes L, Hochman T, Shuman N, Axelrod D, Speyer J, Novik Y. Topical TLR7 agonist imiquimod can induce

immune-mediated rejection of skin metastases in patients with breast cancer. Clinical Cancer Research. 2012 Dec 15;18(24):6748-57. <https://doi.org/10.1158/1078-0432.CCR-12-1149>

- [49] Bahuguna A, Khan I, Bajpai VK, Kang SC. MTT assay to evaluate the cytotoxic potential of a drug. ||| Bangladesh Journal of Pharmacology|||. 2017 Apr 8;12(2):115-8).\
- [50] Parmanik A, Bose A, Ghosh B. Research advancement on magnetic iron oxide nanoparticles and their potential biomedical applications. MINERVA BIOTECHNOLOGY AND BIOMOLECULAR RESEARCH. 2022 Jun 1;34(2):86-95.<https://doi.org/10.23736/S2724-542X.21.02830-3>
- [51] Elmore S. Apoptosis: a review of programmed cell death. Toxicologic pathology. 2007 Jun;35(4):495-516.<https://doi.org/10.1080/01926230701320337>



**Ankita Parmanik**

**Research Scholar**